CHAPTER

13

Anthropogenic Climate Change

13.1 THE WINGS OF DAEDALUS[1]

The greenhouse effect that warms the surface of Earth above its emission temperature results because a few minor constituents absorb thermal infrared radiation very efficiently. As a result of human activities, the atmospheric concentrations of some of these natural greenhouse gases are increasing, and entirely new man-made greenhouse gases have been introduced into the atmosphere. The human-produced increase in the atmospheric greenhouse effect is warming the surface of Earth. When the effects of feedback processes internal to the climate system are taken into account, it becomes clear that human activities are leading to a global climate change that may produce a mean surface temperature on Earth as warm as any for more than a million years. It is one of the great challenges of global climatology to predict future climate changes with adequate detail and sufficiently far in advance to allow humanity to adjust its behavior in time to avert the worst consequences of such a global climate change.

This challenge consists of several interlocking parts. We must first understand and predict the human-induced changes to the environment that are most important for climate, which may include atmospheric gaseous composition, aerosol amount and type, and the condition of the land surface. Then we must predict the climate change that will result from these changed climate parameters. These two steps are not independent, since climate change itself may feed back on the surface conditions and atmospheric composition through physical, chemical, and biological processes.

[1]In Greek mythology Daedalus was an Athenian inventor, architect, and engineer. He was imprisoned with his son Icarus in a tower, but managed to escape by constructing wings from feathers and wax. Icarus was young and imprudent and, despite warnings from his father, flew too close to the Sun, where his wings melted and he fell into the sea and drowned.

Global Physical Climatology. http://dx.doi.org/10.1016/B978-0-12-328531-7.00013-X

13.2 HUMANS AND THE GREENHOUSE EFFECT

Long-lived greenhouse gases that appear to be increasing as a direct result of human activities include carbon dioxide (CO_2), methane (CH_4), nitrous oxide (N_2O), and halocarbons (e.g. CFC-11 and CFC-12). Figure 13.1 shows records of CO_2 and CH_4 from year 1 to 2014, and combines ice core measurements from the Law Dome, East Antarctica, and atmospheric measurements from Cape Grim, Tasmania. The concentrations of these two key greenhouse gases remained approximately constant from year 1 until about 1800, after which they began a rapid increase driven by human activities. This increase accelerated after 1950. The insert shows more detail since the end of preindustrial times, which is generally defined as 1750. In 2014, CO_2 continues on an exponentially increasing trend, but CH_4 began to level off in the 1990s. Methane has increased by a factor of 2.5 since preindustrial times, and it appears that its sinks have begun to balance its sources. Methane has a much shorter lifetime in the atmosphere than carbon dioxide.

Most of the key greenhouse gases that humans are changing have very long lifetimes in the atmosphere so that the amounts we release into the atmosphere today will remain in the atmosphere for up to two centuries, depending on the gas in question (Table 13.1). For each gas in the table (except CO_2), the "lifetime" is defined here as the ratio of the atmospheric content to the total rate of removal. This time scale also characterizes the rate of adjustment of the atmospheric concentrations if the emission rates are changed abruptly. Carbon dioxide is a special case since it has no real

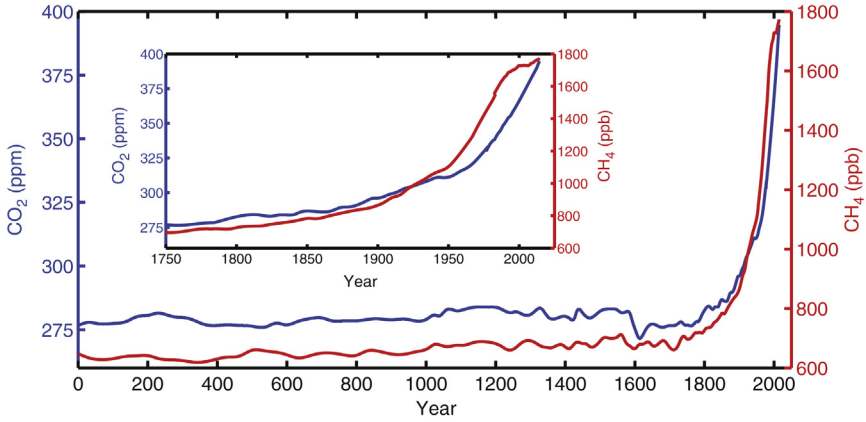

FIGURE 13.1 Carbon dioxide and methane concentrations from ice core measurements at Law Dome, Antarctica, and *in situ* and flask atmospheric measurements from Cape Grim, Tasmania combined together to shown annual means from year 1 to 2014 CE. Insert shows detail since 1750. In situ *data are courtesy of CSIRO and the Australian Bureau of Meteorology. Ice core data are from Etheridge et al. (1996) and MacFarling Meure et al. (2006).*

TABLE 13.1 Characteristics of Some Key Greenhouse Gases That are Influenced by Human Activities

Parameter	CO_2	CH_4	CFC-11	CFC-12	N_2O
Preindustrial atmospheric concentration (1750)	278 ppm	715 ppb	0	0	270 ppb
Current atmospheric concentration (2011)	390 ppm	1803 ppb	238 ppt	527 ppt	324 ppb
Current annual rate of atmospheric accumulation	2.0 ppm (0.5%)	4.8 ppb (0.27%)	−2.25 ppt (−0.93%)	−2.25 ppt (−0.42%)	0.8 ppb (0.25%)
Atmospheric lifetime (years)	(50–200)	10	65	130	150

ppm, parts per million by volume; ppb, parts per billion by volume; ppt, parts per trillion by volume.
Hartmann et al., 2013, Section 2.2.

sinks, but is merely circulated between various reservoirs (atmosphere, ocean, biota). The "lifetime" of CO_2 given in the table is a rough indication of the time it would take for the CO_2 concentration to adjust to changes in the emissions. Simulations of the carbon cycle coupled with climate suggest, however, that the CO_2 increases that we are introducing now will take many centuries to be removed by natural processes and are essentially permanent.

Most of the important greenhouse gases are naturally occurring, but many of the halocarbons are industrially created and have no sources in nature. Although water vapor is the most important greenhouse gas, we exclude it from this discussion because its atmospheric abundance is not under direct human control, but responds freely to the prevailing climate conditions and helps to determine them. The turnover time for atmospheric water vapor is only about 9 days. We consider the changes in long-lived trace species to provide a forcing to the climate system, and we regard the changes in water-vapor abundance that result from this warming to be a feedback process. Nonetheless, we must keep in mind that any temperature change associated with human activity will be composed of a large contribution associated with water-vapor feedback and other feedbacks internal to the climate system. The net effect of all of these feedbacks is not known with great precision (Chapter 10).

13.3 CARBON DIOXIDE

Carbon dioxide is a naturally occurring atmospheric constituent that is cycled between reservoirs in the ocean, the atmosphere, and the land. Figure 13.2 shows how the carbon cycle has been changed by the actions

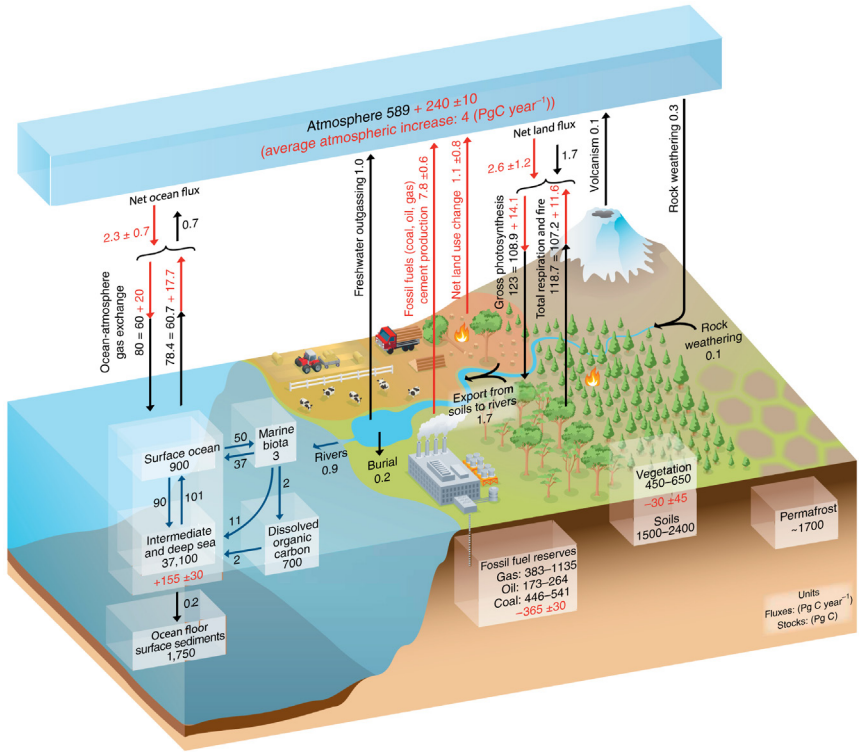

FIGURE 13.2 **Simplified schematic of the global carbon cycle.** Numbers represent reservoir mass, also called "carbon stocks" in PgC (1 PgC = 10^{15} gC) and annual carbon exchange fluxes (in PgC year^{-1}). Black numbers and arrows indicate reservoir mass and exchange fluxes estimated for the time prior to the Industrial Era, about 1750. Red arrows and numbers indicate annual "anthropogenic" fluxes averaged over the 2000–2009 time period. These fluxes are a perturbation of the carbon cycle during Industrial Era post-1750. These fluxes (red arrows) are: fossil fuel and cement emissions of CO_2, net land use change, and the average atmospheric increase of CO_2 in the atmosphere, also called "CO_2 growth rate." The uptake of anthropogenic CO_2 by the ocean and by terrestrial ecosystems, often called "carbon sinks," are the red arrows part of net land flux and net ocean flux. Red numbers in the reservoirs denote cumulative changes of anthropogenic carbon over the Industrial Period 1750–2011. By convention, a positive cumulative change means that a reservoir has gained carbon since 1750. The cumulative change of anthropogenic carbon in the terrestrial reservoir is the sum of carbon cumulatively lost through land use change and carbon accumulated since 1750 in other ecosystems. Note that the mass balance of the two ocean carbon stocks, surface ocean, and intermediate and deep ocean, includes a yearly accumulation of anthropogenic carbon (not shown). Uncertainties are reported as 90% confidence intervals. To achieve an overall balance, the values of the more uncertain gross fluxes have been adjusted so that their difference matches the net land flux and net ocean flux estimates. Fluxes from volcanic eruptions, rock weathering (silicates and carbonates weathering reactions resulting into a small uptake of atmospheric CO_2), export of carbon from soils to rivers, burial of carbon in freshwater lakes and reservoirs, and transport of carbon by rivers to the ocean are all assumed to be preindustrial fluxes, that is, unchanged during 1750–2011. *Figure reproduced from IPCC WG I Report (Fig. 6.1), Ciais et al. (2013), more details and references can be found in Chapter 6. Caption shortened with permission.*

of humans. Fossil fuel reserves are sufficient to continue the current rate of human production of CO_2 for a century or more into the future. CO_2 increased by about 40% between 1750 and 2014 as a result of human activities, about two-thirds of this from fossil fuel combustion and cement manufacture and about one-third from land use change related to changing forest cover (Ciais et al., 2013). About half of the emissions from humans stayed in the atmosphere and about half has been taken up in equal parts by the ocean and the land biosphere. Human emissions of CO_2 have increased in the 2000s and the increase in the first decade of the twenty-first century averaged 2 ppm $year^{-1}$, more rapidly than in any previous decade.

Carbon exchanges rapidly between the atmosphere and the ocean, so that the particular CO_2 molecules in the atmosphere are changed in about 4 years. We may call this the *turnover time*. However, the time required for atmospheric CO_2 to achieve a new equilibrium in response to a perturbation such as fossil fuel burning is much longer, because of the slow rate at which carbon is exchanged between the surface waters and deep ocean. It requires 50–200 years for the atmospheric CO_2 concentration to achieve a new steady state. CO_2 estimates from ice cores indicate that the preindustrial atmosphere maintained a relatively constant CO_2 of about 278 ppmv for centuries. The recent rapid increase in atmospheric CO_2 concentration parallels very closely the known increase in fossil fuel combustion. The fossil fuel origin of the recent CO_2 increase is further confirmed by changes in the isotopic abundance of ^{13}C and ^{14}C. Radiocarbon, the ^{14}C isotope, is created in the upper atmosphere by cosmic rays, and has a half-life of 5570 years. Therefore, since fossil carbon has been buried in the earth for millions of years, it has no radiocarbon. The decrease of about 2% in atmospheric ^{14}C from 1800 to 1950 is consistent with a fossil carbon source. Fossil carbon is also very deficient in ^{13}C because plants strongly favor the lighter isotope, and the decreasing fraction of ^{13}C in CO_2 indicates that the increased CO_2 is coming from organic carbon rather than from a geochemical exchange with the ocean or volcanoes. The decreasing amount of O_2 in the atmosphere is also definitive evidence for fossil fuel combustion as the source of increasing CO_2 in the atmosphere, since O_2 is needed to burn carbon to make CO_2. If fossil carbon fuel consumption increases at current rates, atmospheric CO_2 concentration will be double its preindustrial value by around 2060 and continue to increase after that.

13.4 METHANE

Methane (CH_4) is produced in a wide variety of anaerobic environments, including natural wetlands, rice paddies, and the guts of animals. It is also released during oil and gas drilling and coal mining. At

the present time, it is believed that the human sources of methane from agriculture and waste is about equal to the emissions from natural wetlands, and that anthropogenic emissions are 50–65% of total emissions. The primary removal mechanism is oxidation by hydroxyl (OH) in the atmosphere. Methane oxidation by OH is the dominant source of water vapor in the stratosphere. Water in the stratosphere can be an important greenhouse gas, and both water vapor and ice can influence the photochemistry of ozone.

13.5 HALOCARBONS

Halogens such as chlorine, bromine, and iodine have a wide variety of industrial applications, and in compounds with carbon they produce a number of useful gases. Although present in the atmosphere in very small amounts, industrially produced gases such as CFC-11 (CCl_3F) and CFC-12 (CCl_2F_2) have a substantial influence on the greenhouse effect of Earth. The reason for the strong greenhouse effect of these gases is that they have strong absorption lines in the 8–12-μm region of the longwave spectrum where the surface emission is large. In this wavelength interval, naturally occurring gases do not absorb strongly, so the natural atmosphere is relatively transparent. These gases and other halocarbons are manufactured for use as the working fluid in refrigeration units, as foaming agents, as solvents, and in many other applications. Fully halogenated compounds are extremely unreactive and have very long lifetimes in the atmosphere. They are photodissociated by ultraviolet radiation in the stratosphere, where the chlorine and bromine thus released participate in the catalytic destruction of ozone. Concentrations of these ozone-depleting substances have been decreasing owing to successful international regulation through the Montreal Protocol. Alternatives to fully halogenated compounds are now being used. In their manufacture, one of the halogens is replaced with a hydrogen atom, making the molecules more reactive, giving them shorter lifetimes in the atmosphere, and producing less free chlorine and bromine when they dissociate. The most abundant of these is currently HCFC-22 ($CHClF_2$ ~200 ppt).

13.6 NITROUS OXIDE

Nitrous oxide (N_2O) is produced by biological sources in soils and water. Its primary sinks are in the stratosphere, where it is removed by photolysis and by reaction with electronically excited oxygen atoms. Anthropogenic sources include the use of artificial fertilizers in cultivated soils, biomass burning, and a number of industrial activities.

13.7 OZONE

Ozone (O_3) is increasing in the troposphere and has been depleted in the stratosphere, both owing to human actions. The tropospheric increase is related to industrial and automobile pollution that leads to the photochemical production of ozone near the ground. Ozone in the stratosphere has been depleted by human production of industrial gases such as CFCs, mostly through the action of bromine and chlorine released from them. Ozone near the surface is an environmental hazard because of its health effects on humans and plants. Ozone in the troposphere and lower stratosphere is an effective greenhouse gas, primarily because of the position of its 9.6 μm absorption band in the middle of the water vapor window. When stratospheric ozone recovers in the mid- to late twenty-first century, it will add a little to the greenhouse effect, but not as much as the reduction of CFC-11 and CFC-12 will reduce the greenhouse effect.

13.8 ANTHROPOGENIC AEROSOLS AND CLIMATE

Tropospheric aerosols have direct and indirect effects on the radiation balance, as discussed in Chapter 12. Aerosols directly influence solar and longwave radiative transmission. They also serve as cloud condensation nuclei (CCN), and the abundance of CCN influences the number, size, and atmospheric lifetime of cloud droplets or particles. Cloud abundance and radiative properties have a substantial influence on the net radiation balance of Earth. As discussed in Section 12.3, a big fraction of tropospheric aerosols is produced by conversion of SO_2 gas to sulfate aerosol, and more than half of the total sulfate aerosol production is anthropogenic and mostly related to fossil fuel combustion. These sulfur emissions come mostly from the Northern Hemisphere and have led to a serious problem with acid rain, which motivated successful emission reductions through a cap and trade system in North America that was initiated in 1991, along with the Acid Rain Treaty between Canada and the USA.

It is generally about 1 week between the release of an aerosol precursor gas such as SO_2, its subsequent conversion to sulfate aerosol, and final precipitation in solution within a raindrop. Therefore, the aerosol burden of the troposphere is based on emissions from at most the previous 2 weeks, and if human production of aerosols were to cease, the aerosol burden of the atmosphere would return to its natural level within a similar period. Because of this short lifetime, the aerosol loading of the troposphere is highly variable, and tends to be highest near the sources of aerosols or their precursor gases. Recent trends in aerosol burden have been downward in Europe and North America because of efforts to clean up industrial emissions, and upward in Asia in association with rapid growth in

emissions from coal-powered power plants, factories, and vehicles. Over the long term, the cooling effect of aerosols will be overwhelmed by the warming effect of greenhouse gases. In the near term, though, the difficulty of quantifying the anthropogenic aerosol effect, especially through modification of clouds, imposes a large uncertainty on efforts to use observations of warming to constrain the sensitivity of climate.

13.9 CHANGING SURFACE CONDITIONS

Deforestation in mid-latitudes and the tropics, expansion and contraction of deserts, and urbanization of the landscape can have significant effects on the local surface conditions and local climate. One of the most direct effects is that caused by surface albedo changes, which have a strong influence on the energy balance. When the relatively small fraction of land area on Earth and the effect of cloud cover in screening surface albedo changes are taken into account, however, land surface albedo changes directly caused by humans seem to have a relatively small effect on the global average energy balance, about 0.15 W m^{-2}.

Although land albedo changes may not be of first-order importance for global climate, most people live on continents and the regional climate and ecological changes associated with deforestation and urbanization can be quite important for human populations. It is estimated, for example, that complete removal of the Amazon rain forest would have a substantial influence on local surface temperature and hydrology. About half of the rainfall over the Amazon basin is derived from evapotranspiration from the forest. Removing the forest will change the ratio of runoff to evapotranspiration, and the hydrological balance of the region may be seriously altered. The raised surface albedo also lessens the solar heating that ultimately drives upward motion and low-level moisture convergence. Although model simulations of complex interactions between vegetation and climate are at an early stage of development, some simulations suggest that removing the Amazon rain forest would result in a reduction of both moisture convergence and evapotranspiration, so that runoff would decrease significantly.

13.10 CLIMATE FORCING BY HUMANS

An important contribution of science to the policy options regarding human-induced climate change is to quantify the magnitude of the effect of various human actions in producing global warming. To do this we assume the paradigm that global temperature changes can be divided into a part produced by a forcing and a part contributed by a feedback that depends on the global temperature change. To compute the forcing,

for example, one could take a climate model, leave the temperature, humidity, and clouds unchanged, introduce a change such as increasing the CO_2 from the preindustrial value to today's value, and then compute the change in the top-of-atmosphere (TOA) radiation balance. The change in the radiation balance, thus computed, is then the climate forcing that humans have so far produced by increasing the atmospheric CO_2. Early on, however, it was noted that the stratosphere cools rapidly when the CO_2 is increased, before any surface temperature change has occurred. This change in stratospheric temperature changes the TOA radiation balance and changes the effective forcing of increasing CO_2. To maintain the forcing–feedback paradigm intact, the forcing is now calculated as the change in TOA radiation balance after the stratosphere has come into a new equilibrium with the increased CO_2, but before the surface temperature has changed. A little later, it was discovered that the clouds change rather quickly in response to the CO_2 increase also, as we would expect, since we know that convection is a response to the radiative cooling of the atmosphere, and CO_2 affects the radiative cooling of the atmosphere (Chapter 3). The rapid response of the clouds to CO_2 produces an even larger fast response of the TOA radiation balance and requires another adjustment to the estimate of forcing. To incorporate the fast response of clouds into the forcing from CO_2, one procedure is to introduce the CO_2 change, while keeping the SST fixed in climate model, then run the model long enough so that the clouds have equilibrated to the CO_2 and a new estimate of the effective forcing can be computed. To get stable statistics the model may need to be run for 20 years. The atmospheric temperature and the land temperatures are allowed to respond to the CO_2. The global mean precipitation decreases and shifts a little from the ocean to the land, since the land is allowed to warm and the oceans are not. So the forcing–feedback paradigm has become a little strained in this process, but the goal is to provide the best numbers for use in policymaking. The most recent IPCC report (Stocker et al., 2013) provided a more traditional stratosphere-adjusted radiative forcing (RF), and a cloud-adjusted effective radiative forcing (ERF).

Figure 13.3 shows the temporal evolution of natural and anthropogenic climate forcing from 1750 to 2011 as estimated by the IPCC WG I Fifth Assessment. Values for the major elements of forcing are shown in a bar chart with uncertainty bars on the right. Forcing by CO_2 and other well-mixed greenhouse gases (WMGHG) are large, positive, and relatively certain. Forcings from aerosols and aerosol–cloud interactions are large, negative, and very uncertain, but are thought to offset a significant fraction of the greenhouse gas forcing at the present time. However, aerosol forcing is not changing much at the present time. Total anthropogenic forcing began to increase more rapidly after about 1970 and continues to increase. Forcing from solar variability is small and regular, and volcanic forcing is often large, but is very episodic (Fig. 13.3).

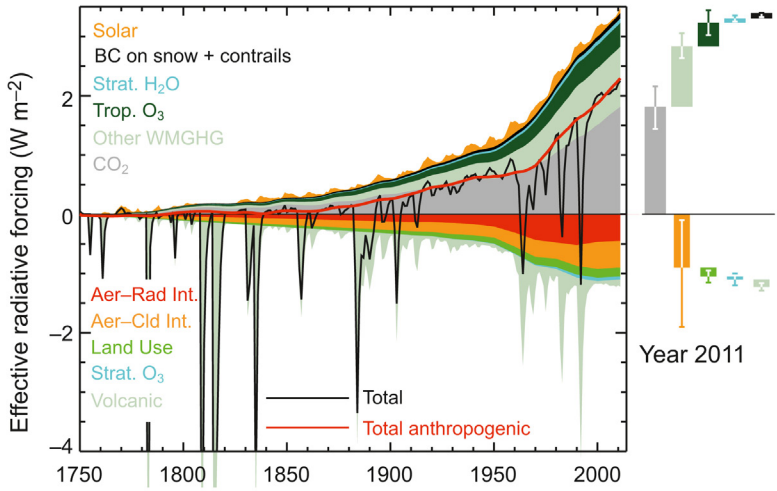

FIGURE 13.3 Time evolution of forcing for anthropogenic and natural forcing mechanisms. Bars with the forcing and uncertainty ranges (5–95% confidence range) at present are given in the right part of the figure. For aerosol the ERF due to aerosol–radiation interaction and total aerosol ERF are shown. The uncertainty ranges are for present (2011 versus 1750). For aerosols, only the uncertainty in the total aerosol ERF is given. For several of the forcing agents, the relative uncertainty may be larger for certain time periods compared to present. The total anthropogenic forcing was 0.57 (0.29–0.85) W m^{-2} in 1950, 1.25 (0.64–1.86) W m^{-2} in 1980, and 2.29 (1.13–3.33) W m^{-2} in 2011. *Figure and caption reproduced from IPCC WG I Report Chapter 8 Fig. 8.18, Myhre et al. (2013) where more details are provided.*

13.11 GLOBAL WARMING POTENTIAL

For planning and regulation purposes it is useful to know the climate impact of a particular human action. For example, "How much warming should we expect from the emission of 1 kg of CO_2?" The answer to this question depends on the climate forcing, as discussed in the previous section, which depends on the efficiency with which one kilogram of CO_2 can reduce the emission of longwave radiation. In addition to this, we need to know how long that extra kilogram of CO_2 will stay in the atmosphere after we have emitted it. This depends on the atmospheric lifetime of the climate forcing in question. These two factors can be combined into the global warming potential, but one must decide over what time frame to integrate the climate forcing. Table 13.2 shows lifetimes, radiative efficiencies, and global warming potentials (GWP) for some long-lived greenhouse gases for time horizons of 20, 100, and 500 years. A good example is methane, which has a much higher radiative efficiency than CO_2, and although its lifetime is much shorter than CO_2, its GWP is higher than that of CO_2, especially on relatively short time scales. The reason we are more

TABLE 13.2 Lifetimes, Radiative Efficiencies, and Global Warming Potentials (GWP) Relative to CO_2

Name	Chemical formula	Lifetime (years)	Radiative efficiency ($W\ m^{-2}\ ppb^{-1}$)	20-year	100-year	500-year
Carbon dioxide	CO_2	50–200	1.4×10^{-5}	1	1	1
Methane	CH_4	12	3.7×10^{-4}	72	25	7.6
Nitrous oxide	N_2O	114	3.03×10^{-3}	289	298	153
CFC-11	CCl_3F	45	0.25	6,730	4,750	1,620
CFC-12	CCl_2F_2	100	0.32	11,000	10,900	5,200
HCFC-22	$CHClF_2$	12	0.2	5,160	1,810	549

CO_2 lifetime is not easily characterized with a single number, and so is shown as a range. The GWP for CO_2 was calculated using a decay time from carbon cycle model.
Numbers were taken from Solomon et al. (2007), Section 2.10.2.

concerned about CO_2 is that there is much more of it in the atmosphere and it is projected to increase much faster, so that its net effect on surface temperature will dominate in the future. Although the 100-year GWP of methane is 25 times that of CO_2, the annual increase of CO_2 is 400 times that of methane (Table 13.1). Similarly HCFC-22 has a massive GWP compared to CO_2, but its concentration in the atmosphere is tiny, so its effect on climate is currently small and will likely remain so until after CO_2 has greatly warmed the surface. Nonetheless, the warming effect of methane is currently more than a third of that of CO_2 and it has a relatively short lifetime in the atmosphere. So if you wanted to produce a quick reduction in greenhouse gas forcing, one way might be to reduce methane emissions, since the methane would begin to decline quickly and the reduction in greenhouse gas forcing would be significant.

13.12 EQUILIBRIUM CLIMATE CHANGES

A standard experiment with a global climate model is to calculate the equilibrium climate for present and for doubled atmospheric carbon dioxide concentrations and study the differences between the two climate states. In such studies, the transient nature of the carbon dioxide increase and the climate response are ignored and only the state of the climate system when it is in balance with a particular concentration of CO_2 is considered. The response of the equilibrium climate to doubled CO_2 is easier to compute than the transient response and gives useful information about

the nature of the transient climate response to be expected. Doubled CO_2 is used as a surrogate for an equivalent climate forcing that may consist of contributions from many greenhouse gases.

13.12.1 One-Dimensional Model Results

A simple estimation of the response to changed greenhouse gases or other radiative forcings can be obtained from one-dimensional radiative–convective equilibrium models (Section 3.10). The vertical temperature profiles from such calculations for changed CO_2 concentration and changed total solar irradiance (TSI) are shown in Fig. 13.4. These calculations were performed for average cloudiness, fixed relative humidity, and a moist adiabatic lapse rate. Notice that for a CO_2 increase and a TSI increase the surface warming is similar, but that the temperature change in the stratosphere is opposite, warming in the case of increased TSI and cooling in the case of CO_2 increase. Surface temperature increases with CO_2 concentration because of its enhancement of the total greenhouse effect, but the stratospheric temperatures decline with increasing CO_2. The reasons for this can be easily understood by remembering that the approximate stratospheric energy balance is between heating through absorption of solar radiation by ozone and cooling by emission from CO_2 (Fig. 3.18).

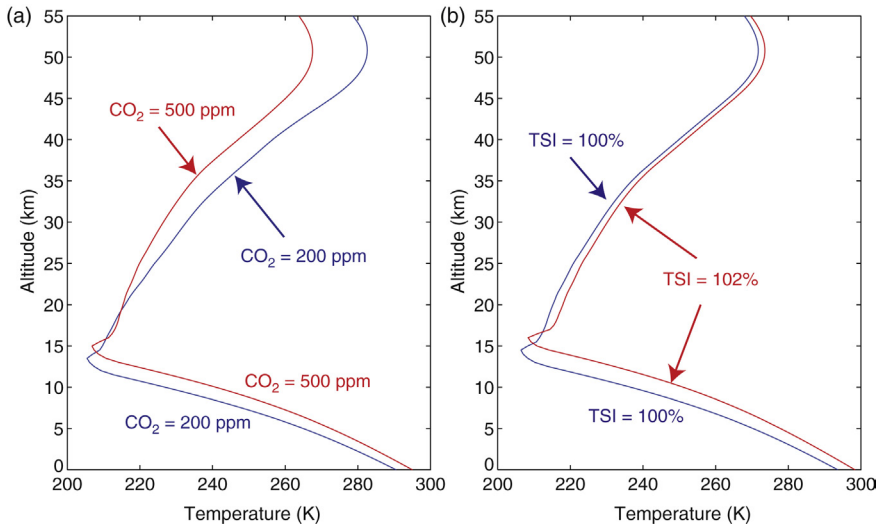

FIGURE 13.4 Radiative–convective equilibrium temperature profiles computed with a one-dimensional model with a moist adiabatic lapse rate. (a) CO_2 concentrations of 200 ppm and 500 ppm and (b) total solar irradiance of 100% and 102% of the current value.

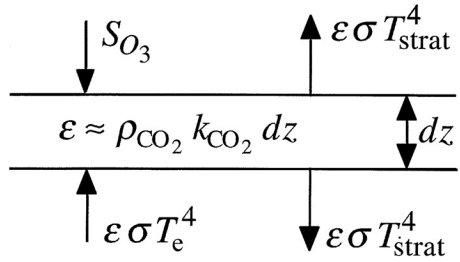

FIGURE 13.5 **Diagram showing the energy fluxes for a thin layer of stratospheric air in which ozone absorbs an amount of solar radiation S_{O_3}, and that absorbs and emits terrestrial radiation with an emissivity of $\varepsilon \ll 1.0$.**

We can illustrate the dependence of stratospheric temperature on its longwave emissivity through a very simple model (Fig. 13.5). Suppose that we consider a thin layer of the stratosphere with a longwave emissivity that is much less than 1 ($\varepsilon \ll 1.0$). This layer will absorb a fraction of the outgoing longwave radiation, and it will emit up and down according to its assumed emissivity. In addition, it will receive solar heating through the absorption by ozone S_{O_3}. The absorption by this layer of solar and outgoing longwave radiation (σT_e^4) must be balanced by its longwave emission.

$$S_{O_3} + \varepsilon\sigma T_e^4 = 2\varepsilon\sigma T_{\text{strat}}^4 \tag{13.1}$$

Solving for the temperature of the stratospheric layer shows the relationship of the stratospheric temperature to the emissivity of the layer.

$$T_{\text{strat}} = \sqrt[4]{\frac{\varepsilon^{-1} S_{O_3} + \sigma T_e^4}{2\sigma}} \tag{13.2}$$

Since CO_2 is the principal longwave absorber in the middle and upper stratosphere, and from (3.29) $\varepsilon \approx \rho_{CO_2} k_{co_2} dz$, we know that the emissivity would increase when the CO_2 concentration is doubled. If we assume that the ozone amount and the planetary albedo remain unchanged when the CO_2 concentration is increased, then the absorbed solar radiation and the outgoing longwave radiation will be the same for a doubled CO_2 climate in equilibrium. Therefore, nothing within the radical in (13.2) will change except the emissivity of the stratospheric layer, and the stratospheric temperature will decline with increasing CO_2.

Figure 13.4 shows that the vertical structure of the warming response for a CO_2 increase and a TSI increase are different. This is also true for the latitude structure of the response, since a TSI change will produce a stronger radiative forcing in the Tropics, whereas the radiative forcing from a CO_2 increase may actually be stronger in high latitudes, since the fractional

increase in the greenhouse effect is larger in high latitudes where much less water vapor is present to compete with CO_2 in absorbing longwave radiation. The effective radiative forcing adjustment for CO_2 and TSI are also different, since CO_2 warms the atmosphere and suppresses clouds, whereas a TSI increase heats the surface more than the atmosphere and enhances clouds. So the rapid adjustments to CO_2 forcing and TSI forcing are also different.

13.13 DETECTION AND ATTRIBUTION

Climate science has been able to answer two very key questions regarding climate change. These are, *detection*: "Is the surface of Earth warming?" and *attribution*: "Are humans causing the surface of Earth to warm"? To answer the detection question it must be shown that the warming that has been observed over the past century cannot be explained as change that has resulted from natural internal variability of the climate system, or from natural forcing such as volcanoes or solar variability. To answer the attribution question, it must be shown that the observed warming could not have occurred without the climate forcing that humans have provided. These questions are answered in the affirmative with multiple lines of observational evidence and with many experiments with global climate models.

Independent instrumental temperature records all indicate warming. Surface air from land stations and ocean observations, upper air from balloons and satellites, sea surface temperature from *in situ*, and satellite measurements and ocean heat content are all warming. In addition, other instrumental records are also showing change that is consistent with warming. Atmospheric specific humidity is increasing, Arctic sea ice is declining, mountain glaciers are shrinking, and sea level is rising. Careful work with data and climate models has indicated that most of these changes are unlikely to have occurred without the warming associated with the production of greenhouse gases by humans.

Figure 13.6 illustrates the method by which climate models are used to confirm detection of global warming and attribution of warming to humans. On the left are the observed global mean temperatures in black, along with the global mean temperature from a large suite of model simulations from CMIP3 and CMIP5, the model integrations done for the IPCC 4th and 5th assessments, respectively (Taylor et al., 2012). These integrations were done separately with the best estimate of only the natural climate forcings and with the best estimate of the natural plus anthropogenic forcings. Fig. 13.6a shows that none of the model experiments can simulate the warming after 1980 if only the natural forcings are included, whereas if the human forcing is included the models can simulate the warming after

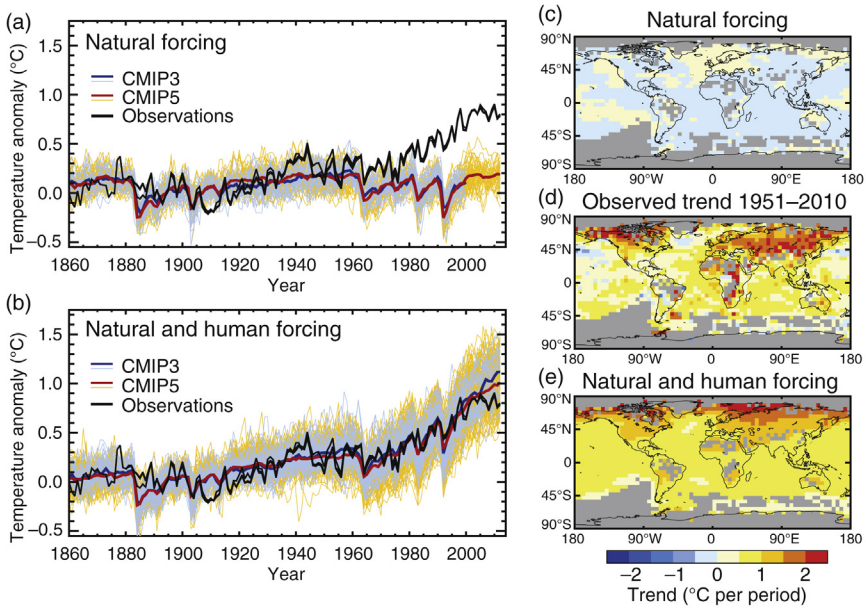

FIGURE 13.6 (Left) Time series of global and annual averaged surface temperature change from 1860 to 2010. (a) The results from two ensemble of climate models driven with just natural forcings, shown as thin blue and yellow lines; ensemble average temperature changes are thick blue and red lines. Three different observed estimates are shown as black lines. (b) The simulations by the same models, but driven with both natural forcing and human-induced changes in greenhouse gases and aerosols. (Right) Spatial patterns of local surface temperature trends from 1951 to 2010. (c) The pattern of trends from a large ensemble of Coupled Model Intercomparison Project Phase 5 (CMIP5) simulations driven with just natural forcings. (d) The pattern of observed trends from the Hadley Centre/Climatic Research Unit gridded surface temperature data set 4 (HadCRUT4) during this period. (e) The trends from a corresponding ensemble of simulations driven with natural + human forcings. *Figure and caption reproduced exactly from IPCC WG I Report Chapter 10 Fig. FAQ 10.1 Figure 1, Bindoff et al. (2013).*

1980 very well. The conclusion is that the warming after 1980 would not have happened without humans. Some of the earlier warming also seems to have been caused by humans, but it was not yet big enough to exceed the natural year-to-year variability of global annual mean temperature. On the right in Fig. 13.6 are maps of the surface temperature trends from 1951 to 2010 as observed, as modeled with only natural forcing and as modeled with human forcing included. The models suggest that without humans the climate would have cooled slightly from 1951 to 2010, mostly as a result of volcanic eruptions, but that with human forcing included the magnitude and pattern of warming produced by the models is similar to the observed warming. Such analyses have also been used to attribute other changes to human influences, including warming on all continents

except Antarctica, the cooling of the stratosphere, the warming of the upper oceans, sea level rise, and Arctic sea ice decline (Bindoff et al., 2013).

13.14 TIME-DEPENDENT CLIMATE CHANGES

The changes in climate that result from human activities occur gradually in response to steadily increasing climate forcing by greenhouse gas increases, aerosol production, and land surface modification. The transient response of the climate system to the anthropogenic shift in climate forcing may be very different from the equilibrium response, and equilibrium may never be achieved since it is unlikely that the anthropogenic forcing of climate will remain constant for the many centuries required for a steady state to be established. Moreover, the immediate need is to understand the history of climate that we are likely to experience over the next 100 years or so given a particular climate-forcing scenario. The response of the climate system to changed thermal forcing will be delayed by the large heat capacity of the ocean. In addition, the ocean currents and their slow response to this thermal forcing may yield geographic variations in the temperature change that are different from those of an equilibrium calculation. The ocean model is thus critical to the prediction of the transient and equilibrium response to climate forcing.

Much of the initial lag of the warming behind the forcing is associated with storage of heat in the ocean mixed layer. The response of the mixed-layer ocean models can be understood using very simple conceptual models. In these models, the ocean is represented by a wet surface with the heat capacity of the mixed layer of the ocean. We may represent the global mean transient temperature response T' to an imposed climate forcing, Q, with a first-order differential equation.

$$c\frac{dT'}{dt} = -\lambda_R^{-1}T' + Q \tag{13.3}$$

The time tendency term on the left represents the storage of energy in the ocean, c is the heat capacity of the ocean, and λ_R is the climate sensitivity parameter defined in (10.2). The solution to (13.3) for the case in which the temperature perturbation is initially zero is easily obtained.

$$T' = e^{-t/\tau_R}\int_0^t c^{-1}Qe^{t'/\tau_R}dt' \tag{13.4}$$

The response time, $\tau_R = c\lambda_R$, is proportional to the product of the heat capacity of the system times the sensitivity parameter. This makes it difficult to estimate the equilibrium climate change from the initial history of an induced warming, since both the sensitivity and the effective heat capacity are uncertain. Both the magnitude of the equilibrium response

and the time required to achieve it are proportional to λ_R. The system (13.3) with formal solution (13.4) has only two independent parameters. So if you have a solution for an initial set of parameters c_1, Q_1 and λ_{R_1}, the solution will be exactly the same for a different sensitivity, λ_{R_2}, so long as you choose the forcing and heat capacity such that,

$$Q_2 = Q_1 \frac{\lambda_{R_1}}{\lambda_{R_2}} \text{ and } c_2 = c_1 \frac{\lambda_{R_1}}{\lambda_{R_2}} \tag{13.5}$$

So one temperature history can be produced by an infinite number of combinations of c, Q and λ_R.

If the perturbation temperature is forced by an instantaneous switch-on of steady forcing

$$Q = \begin{cases} 0, & t \le 0 \\ Q_0, & t > 0 \end{cases} \tag{13.6}$$

where Q_0 is a constant, the solution (13.4) becomes

$$T' = \lambda_R Q_0 (1 - e^{-t/\tau_R}) \tag{13.7}$$

so that the equilibrium temperature perturbation $T' = \lambda_R Q_0$ is approached exponentially with an e-folding time scale of τ_R.

For CO_2 increasing exponentially with time, the change of climate forcing is approximately linear with time, because the radiative forcing scales approximately as the logarithm of CO_2 concentration. If we apply a forcing that increases linearly in time

$$Q = \begin{cases} 0, & t \le 0 \\ Q_t t, & t > 0 \end{cases} \tag{13.8}$$

and insert it into the solution (13.4) for (13.3), we obtain

$$T' = \lambda_R Q_t \{t + \tau_R (e^{-t/\tau_R} - 1)\} \tag{13.9}$$

The exponential term within the brackets represents an initial transient, which for $t >> \tau_R$ is small compared to the other two terms, after which time the solution becomes approximately

$$T' \approx \lambda_R Q_t \{t - \tau_R\} \tag{13.10}$$

The forcing at any time is $Q_t t$ to which the equilibrium response would be $\lambda_R\ Q_t\ t$. From (13.10), we infer that the transient response to linearly increasing forcing is just the equilibrium response, delayed by

the response time τ_R. Choosing the thermal capacity to be that of 150 m of water [$c = 7.3 \times 10^8$ J K^{-1}m^{-2} from (4.5)] and choosing the sensitivity parameter to be such that doubling CO_2 leads to an equilibrium response of 4°C ($\lambda_R = 1$ K (W m^{-2})$^{-1}$), yields a response time of $\tau_R = 20$ years. The response of this simple model to linearly increasing forcing is similar to the global mean response of a GCM with a mixed-layer ocean. The transient response is very much like the equilibrium response, except delayed by about 20 years. The temperature responds sooner over the continental interiors where the effect of the ocean's heat capacity is less directly felt.

The simple model (13.3) has three independent parameters that determine the structure of the transient climate response: the forcing, the heat capacity, and the climate sensitivity. The real-world value of each of these parameters is uncertain, and we can use this model to illustrate why the global mean temperature record does not help to constrain these parameters very well. Figure 13.7a shows example solutions for a forcing that increases linearly at a rate of 4 W m^{-2} per 70 years, approximately the rate of increase of human forcing by greenhouse gas emissions. Solutions are shown with climate sensitivities that differ by a factor of two and mixed layer heat capacities that vary inversely with the sensitivity to keep the time scale $\tau_R = c\lambda_R$ constant. For the first 50 years, these two simulations are virtually indistinguishable, certainly within the observational precision, but they diverge greatly in the second half of the century, when the more sensitive climate warms much more. Therefore, even if the forcing was precisely known, which it is not, the temperature record would not allow us to constrain the sensitivity to within a factor of two, if the rate at which the ocean will take up heat is also uncertain. Figure 13.7b shows the

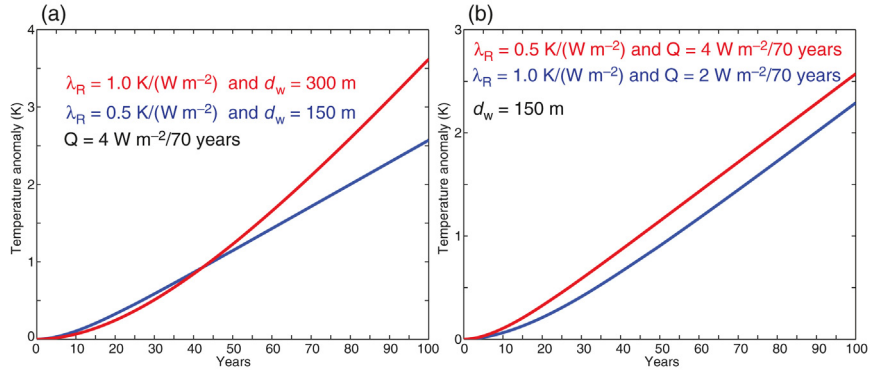

FIGURE 13.7 **Response of a simple climate model to linearly increasing forcing from equation (13.9).** (a) Forcing increasing 4 W m^{-2} per 70 years, comparing doubled sensitivity and doubled mixed-layer depth (red) with baseline values (blue). (b) Mixed-layer depth of 150 m, but comparing doubled sensitivity and halved forcing (red) with baseline values (blue).

case where we assume we know the heat capacity very well, but the forcing and the sensitivity are both uncertain. In this case, the more sensitive model jumps out to an early lead, but because the equilibrium climate sensitivity is the same, the two models maintain the same rate of warming once the initial transient has died away. If the sensitivity and the forcing errors compensate, then the rate of warming is the same, despite the time scale for adjustment being different. So the uncertainty in each of heat capacity, sensitivity, and forcing precludes any of them being constrained very precisely by the observational record, even though we can establish detection and attribution with a high degree of confidence.

In atmosphere–ocean climate model simulations with dynamically active oceans, the timing and spatial structure of the response are more complex. When ocean currents are included in the simulation, the warming is much reduced around Antarctica and over the north Atlantic (Fig. 11.15), where mixing with the deep ocean occurs. Ocean models have two time scales, a rapid adjustment of the mixed layer, and a much longer time scale of hundreds of years associated with the deep circulation of the ocean (Held et al., 2010). Also, it is reasonable that the sensitivity of climate is not constant, as sensitivity is a property of the mean climate. A simple example is surface ice. When less surface ice is present, the surface ice feedback is reduced.

13.15 PROJECTIONS OF FUTURE CLIMATE

It is very important to predict how the climate will change in the future. Robust projections of future climate can be used to plan actions that will reduce the impact of climate change on the natural and built environment, either by reducing positive climate forcing, or by adapting to the changes that will occur. To make useful projections for more than several decades into the future, it is necessary to specify the actions that humans will take that affect the climate. For the IPCC Fifth assessment, four Representative Concentration Pathways (RCPs) were defined in order to cover the likely spread of possible future human emissions of greenhouse gases (van Vuuren et al., 2011). They are named after the approximate anthropogenic human forcing in the year 2100, which are (+2.6 W m^{-2}, +4.5 W m^{-2}, +6.0 W m^{-2}, +8.5 W m^{-2}). The resulting CO_2 concentrations are shown in Fig. 13.8. The lowest emission scenario is RCP 2.6, which represents a reduction in greenhouse gas emissions sufficient to keep global mean warming under about 2°C. It stabilizes CO_2 at about 450 ppm by about 2075. The highest emission scenario, RCP 8.5, represents the path we are currently on, sometimes called the "business as usual" scenario. For RCP 8.5, the CO_2 reaches 1000 ppm shortly after 2100. Other greenhouse gases besides CO_2 are expected to contribute to

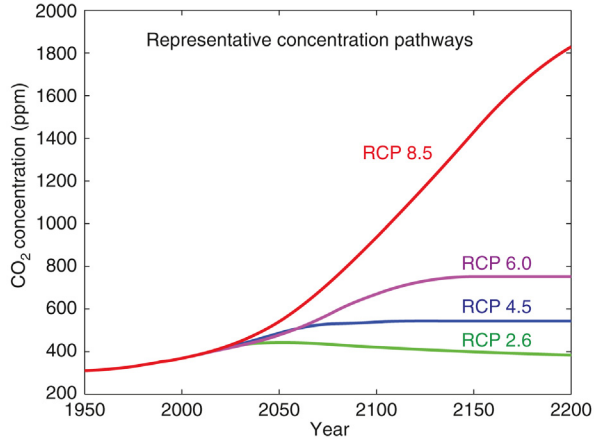

FIGURE 13.8 **Past and projected CO_2 concentrations for the four representative concentration pathways utilized by the IPCC Fifth Assessment to project possible future climates.**

future warming. When the effect of these other greenhouse gases are incorporated and translated into an equivalent CO_2 concentration, the CO_2 equivalent exceeds 1300 ppm when the actual CO_2 reaches 1000 ppm. To move from the RCP 8.5 scenario we are currently following to any of the lower emissions scenarios requires a rapid reduction in CO_2 emissions, most especially from fossil fuel combustion. This could be achieved through a combination of increased efficiency, shifting to energy sources such as solar, wind and nuclear, and carbon capture and storage at fossil fuel power plants.

The response of the global mean surface temperature to these climate forcing scenarios is uncertain, especially because of uncertainty in the climate feedbacks described in Chapters 10 and 11. Figure 13.9a shows projected changes in global mean surface temperature for the RCP 2.6 and RCP 8.5 scenarios, plus the uncertainty in these projections, which is large because the forcing, feedback, and ocean storage rate are all somewhat uncertain. The best estimates for 2200 are about 2°C for RCP 2.6 and 6°C for RCP 8.5. Some of the expected impacts of RCP 8.5 were described in Chapter 11, especially changes in the hydrologic cycle in Fig. 11.14, and the spatial distribution of warming in Fig. 11.15. Changes in the hydrologic cycle will be very significant, with the intensity of both floods and droughts increasing as the spatial and seasonal contrasts in the hydrologic cycle are increased. Global average precipitation will increase at 1–3% per Kelvin of warming, but not as fast as the specific humidity, which will go up at about the Clausius–Clapeyron rate 6–7% K^{-1}. In regions of moisture convergence, the precipitation may go up at faster than the

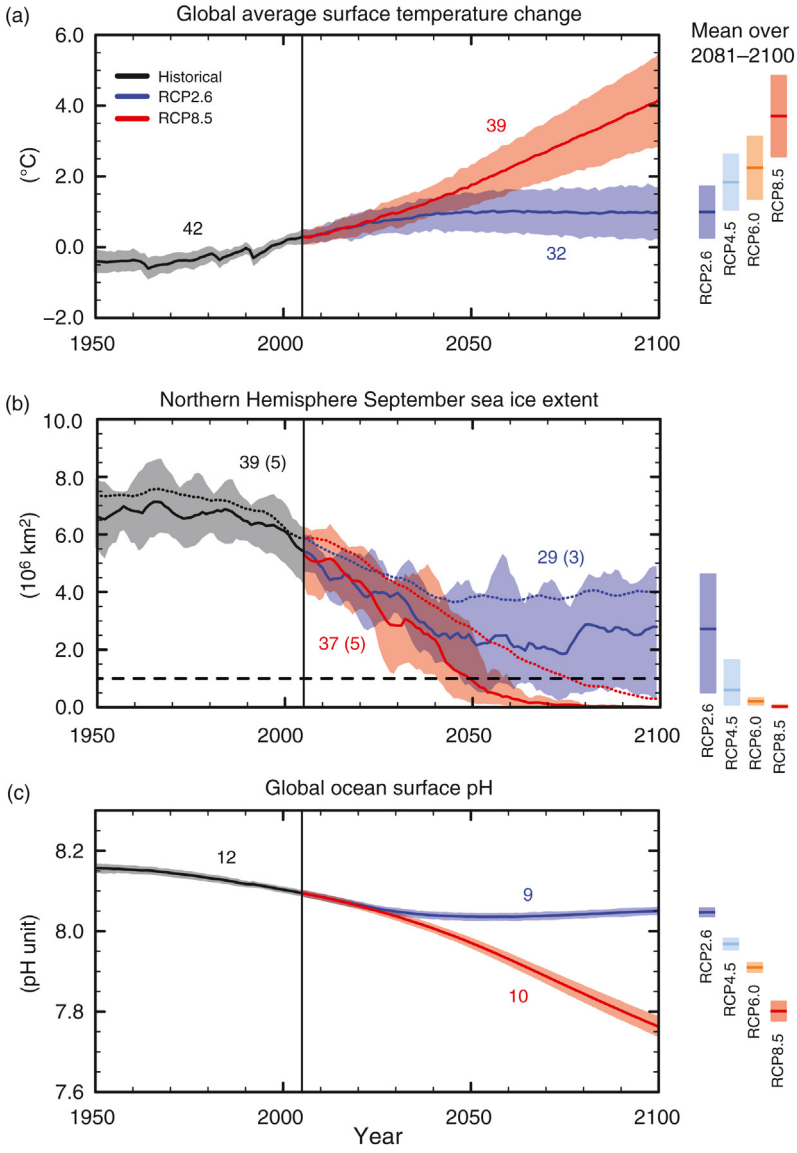

FIGURE 13.9 CMIP5 multimodel simulated time series from 1950 to 2100 for (a) change in global annual mean surface temperature relative to 1986–2005, (b) Northern Hemisphere September sea ice extent (5-year running mean), and (c) global mean ocean surface pH. Time series of projections and a measure of uncertainty (shading) are shown for scenarios RCP 2.6 (blue) and RCP8.5 (red). Black (gray shading) is the modeled historical evolution using historical reconstructed forcings. The mean and associated uncertainties averaged over 2081–2100 are given for all RCP scenarios as colored vertical bars. The numbers of CMIP5 models used to calculate the multi-model mean is indicated. For sea ice extent (b), the projected mean and uncertainty (minimum–maximum range) of the subset of models that most closely reproduce the climatological mean state and 1979–2012 trend of the Arctic sea ice is given (number of models given in brackets). For completeness, the CMIP5 multimodel mean is also indicated with dotted lines. The dashed line represents nearly ice-free conditions (i.e., when sea ice extent is less than 10^6 km^2 for at least 5 consecutive years). *Figure and caption reproduced exactly from IPCC WG I Report Summary for Policymakers Fig. SPM.7, Stocker et al. (2013).*

Clausius–Clapeyron rate, but in other regions it will need to go up much more slowly or even decrease to satisfy the atmospheric energy balance.

Models and observations indicate that warming will be greater in high latitudes and will have a very visible impact on the landscape through the reduction in snow cover, sea ice and the melting of permafrost. The reduction in Arctic Sea ice has been dramatic over the period of satellite observation. Current models vary greatly in their projections of sea ice, and the future of sea ice is regarded as uncertain, but models that produce the most realistic current sea ice conditions predict that the Arctic will become ice free by about 2050 under the RCP 8.5 scenario (Fig. 13.9b). Under RCP 2.6, a minimum of 2 million square kilometers of sea ice in September is maintained through 2100. Another important impact of CO_2 increase is acidification of the ocean. CO_2 dissolved in water forms carbonic acid, the sharp taste of carbonated beverages, which lowers the pH of seawater. Sea life is adapted to basic water, particularly organisms that form calcite shells. Increased CO_2 in the atmosphere is thus a threat to organisms that form the base of the food chain in the ocean. The RCP 8.5 scenario produces a stronger reduction in ocean pH and so a more acidic ocean (Fig. 13.9c), providing another motivation to reduce emissions of CO_2.

Sea ice concentrations have declined during the period of satellite observations more rapidly than most models predicted, but it is uncertain whether the sea ice was not sensitive enough to warming in the current generation of models or whether natural variability has added onto the recent decline of Arctic Sea ice forced by anthropogenic warming. The year-to-year variability of Arctic sea ice extent is fairly large. Figure 13.10 shows the satellite-measured Arctic sea ice area and sea ice extent during

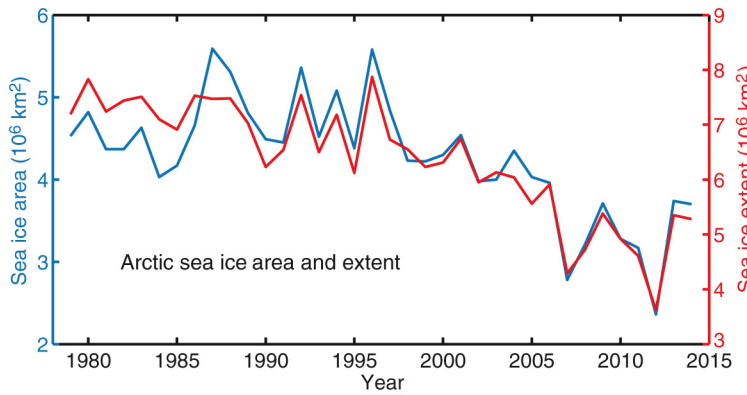

FIGURE 13.10 **Arctic sea ice area and extent during September from NASA passive microwave satellite records from 1979 through 2014.**

September from 1979 to 2014. Satellite microwave measurements are used to make an estimate of the fraction of the ocean surface that is sea ice in an area. If the concentration is over the threshold of 15%, then sea ice is defined to be present. Sea ice extent is the total area where ice is present, and September sea ice extent averaged about 7 million square kilometers in the Arctic from 1979 to 1996. The sea ice area is the product of the area of a geographic grid box and the sea ice concentration in that box, summed over the Arctic or Antarctic. The extent is thus always greater than the area, but it also seems to be a little more stable from year-to-year, especially early in the record. Both area and extent show a period of little trend before about 1996, and a significant downward trend after that (Cavalieri and Parkinson, 2012). The year with the least sea ice extent in this period was 2012, when the extent was about 3.5 million square kilometers, compared to 7 in the early record, or a decline of 50%, which is far outside the range of variability earlier in the record.

Figure 13.11 shows the daily sea ice extent for each year from 1979 to 2014. The first 7 years (1979–1985) are plotted in blue and the last 7 years (2007–2014) are plotted in red. In the Arctic the sea ice extent appears to have been reduced in every season, but most notably in September, the month of minimum Arctic sea ice extent. In the Antarctic the sea ice trends have been smaller, but in all seasons the sea ice extent appears to have increased a little over this period, contrary to the predictions of climate models (Parkinson and Cavalieri, 2012). In the long run, sea ice extent is expected to decline with global warming, so it is likely that the Antarctic sea ice increase during this period is a product of natural variability, perhaps related to the trend toward more La Niña-like conditions that was discussed in Chapter 8. It has also been hypothesized that melting of glacier ice has freshened the surface water around Antarctica, allowing

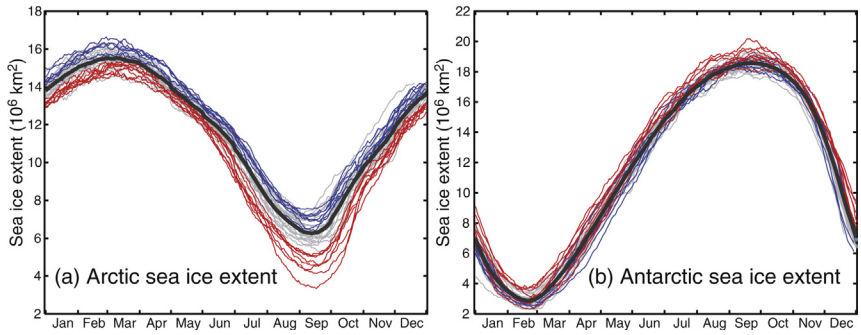

FIGURE 13.11 **Annual cycles of daily (a) Arctic and (b) Antarctic sea ice extent.** 2007–2014 are shown in red, while 1979–1985 are shown in blue. All other years are shown in gray. *NASA satellite data.*

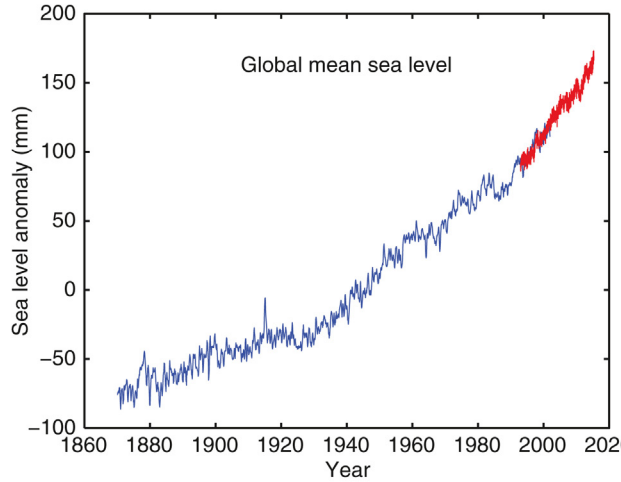

FIGURE 13.12 Global mean sea level anomalies from gauge data (blue, 1870–2001) and from satellite altimetry measurements (red, 1999–2014). Satellite data have been adjusted to have the same mean as the gauge data during the period of overlap. *Gauge data are from Church and White (2011) and satellite data from Nerem et al. (2010).*

sea ice to form farther from the coast (Hansen et al., 2015), so that the Antarctic sea ice expansion is a transient response to human-induced changes in the climate system.

One of the more significant impacts of human-induced global warming is sea level rise. Estimates from tide gauges suggest that the global sea level has risen by about 19 cm from 1901 to 2010 (Fig. 13.12). Between 1993 and 2010, the rate of sea level rise was about 3.2 mm year^{-1}, which is faster than the average rise over the past century. This rise in sea level parallels the rise in temperature over this period. Evidence from paleo sea level evidence for the past 3 million years suggests that sea level was 5 m higher in the past when the temperature was about 2 K warmer than present.

The major contributors to sea-level rise over the period of satellite observation (1993–2010) are: thermal expansion of the ocean (~ 40%), melting of mountain glaciers and small ice caps (~ 30%), and melting of the Greenland and Antarctic Ice Sheets (~ 25%) (Church et al., 2013). Recent evidence suggests an acceleration of Greenland Ice Sheet melting, and observations and models also suggest that some ice sheets in West Antarctica that are grounded below sea level are unstable and will eventually flow into the ocean, adding to sea level rise (Joughin et al., 2014; Rignot et al., 2014). Many glaciologists believe it is plausible that the Greenland ice sheet will melt away if the human-induced warming exceeds 2°C, but it is likely that it will take centuries to completely melt. If this happens the sea level rise will be about seven meters.

The future behavior of the major ice sheets is more uncertain than the thermal expansion of the ocean in response to warming. Projections of sea level rise over the next century are 26 to 53 cm for the RCP 2.6 scenario and 52 to 98 cm for RCP 8.5. For RCP 8.5 the rate of seal level rise in 2090 would be 8 to 16 mm $year^{-1}$, about 4–8 times the average rate during the twentieth century (1.7 mm $year^{-1}$) (Church et al., 2013).

13.16 OUTLOOK FOR THE FUTURE

It is very clear that human activities have altered the atmosphere and that if we continue to release CO_2 and other greenhouse gases we can produce a climate warmer than any for the past million years. The magnitude and timing of this global climate change are both uncertain and depend on economic and social decisions that society has yet to make. The key question is whether we will continue to burn fossil carbon energy sources and release the combustion products into the atmosphere. Figure 13.13 shows the projected warming of global mean surface temperature since 1870 as a function of the total CO_2 emissions since 1870. All 4 of the RCP scenarios are shown, and all fall along the same line. This means that for the global mean surface temperature increase it matters little at what rate we release CO_2, but only the total amount of CO_2 that is released. Also of note is that in 2010 we were about half way to the amount of CO_2 emission that will lead to a 2°C warming. Scientific evidence and some treaty agreements under the United Nations Framework Convention on Climate Change both indicate 2°C as the level of warming that becomes "dangerous" with respect to its potential impacts, nonlinearities and uncertainties. Under the RCP 8.5 scenario, the one we are currently following, we will reach this dangerous level by 2040, just 25 years from the time of this writing. Under the RCP 2.6 scenario, dangerous warming is averted.

Energy production from renewables like solar and wind have been increasing rapidly, but are still small compared to fossil fuel energy, which made up 82% of world energy production in 2012. Fossil fuel reserves are large and energy production from fossil fuels has increased very rapidly in the early twenty-first century. Global mean surface temperature has increased about 0.8°C in the past century, mostly because of fossil fuel burning, and another 0.5°C will occur if no further greenhouse gas additions are made, since the warming lags behind the climate forcing. So while it is technically possible to reduce emissions through a variety of means and achieve a stabilization of climate as envisioned in the RCP 2.6 scenario (e.g. Pacala and Socolow, 2004), the world has continued on the path of rapid fossil fuel exploitation, with every indication that efforts to mitigate global warming will be too little and too late when they finally occur.

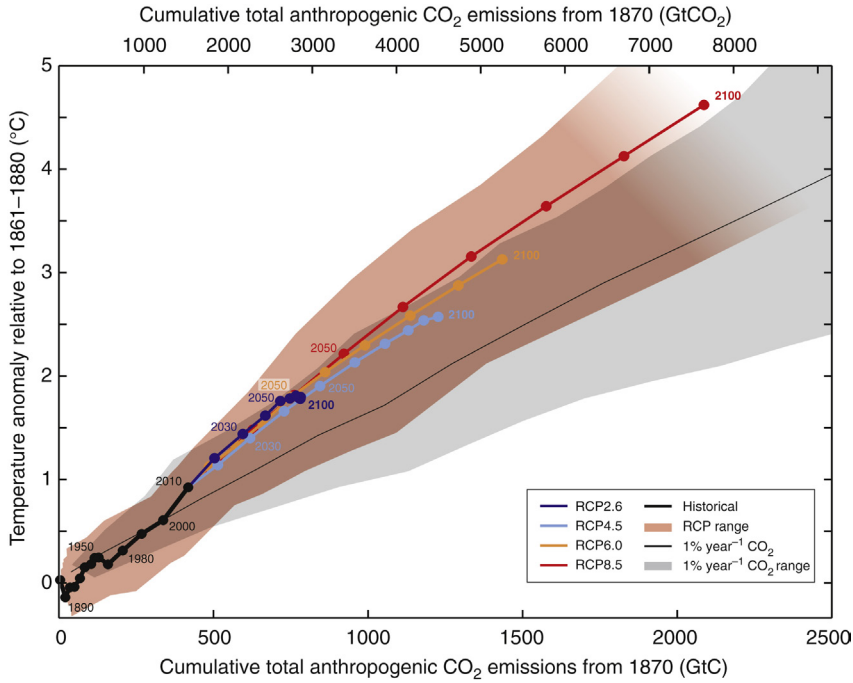

FIGURE 13.13 Global mean surface temperature increase as a function of cumulative total global CO_2 emissions from various lines of evidence. Multimodel results from a hierarchy of climate-carbon cycle models for each RCP until 2100 are shown with colored lines and decadal means (dots). Some decadal means are labeled for clarity (e.g., 2050 indicating the decade 2040–2049). Model results over the historical period (1860 to 2010) are indicated in black. The colored plume illustrates the multi-model spread over the four RCP scenarios and fades with the decreasing number of available models in RCP8.5. The multi-model mean and range simulated by CMIP5 models, forced by a CO_2 increase of 1% per year (1% year^{-1} CO_2 simulations), is given by the thin black line and gray area. For a specific amount of cumulative CO_2 emissions, the 1% per year CO_2 simulations exhibit lower warming than those driven by RCPs, which include additional non-CO_2 forcings. Temperature values are given relative to the 1861–1880 base period, emissions relative to 1870. Decadal averages are connected by straight lines. *Figure and caption reproduced exactly from IPCC WG I Report Summary for Policymakers Fig. SPM.10, Stocker et al. (2013).*

13.17 CLIMATE INTERVENTION: GEOENGINEERING THE CLIMATE OF EARTH

It is technically feasible to mitigate global warming by reducing the emissions of greenhouse gases while still maintaining growth in global energy consumption, and this is likely the best option. Since moving to a low CO_2 emission pathway has proved difficult for political, economic and social reasons, it has been proposed that we consider interventions to mitigate the warming produced by our introduction of greenhouse gases

into the atmosphere. These actions fall into two broad categories: increasing the albedo of Earth, and removing CO_2 from the atmosphere after it has been introduced.

We have already seen several examples of how nature or humans have increased the albedo of Earth. One way is to inject aerosol precursor gases like SO_2 into the stratosphere to simulate the cooling that a major volcanic eruption produces. This is technically and economically feasible. Another way is to increase the albedo of clouds in the marine boundary layer by introducing cloud condensation nuclei. So far, this seems less technically feasible. A major problem with these approaches is that they would have to be maintained in perpetuity, since if they were ever stopped a large and rapid warming would occur. Also, enhanced CO_2 in the atmosphere is making the ocean more acidic, with potentially serious consequences for the ocean food chain. Cooling the Earth by reflecting more solar radiation would not stop the acidification of the ocean. In addition, increasing the albedo of Earth while increasing the CO_2 of the atmosphere would change the driving of convection and could lead to shifts in the amount or distribution of precipitation and evaporation (e.g. Fig. 13.4). Albedo modification strategies do not address the root cause of human-induced warming, which is greenhouse gas increases, and they may raise additional risks, but they are relatively cost-effective and could produce significant cooling within a few years.

CO_2 removal strategies focus on increasing the rate of carbon uptake by the ocean or land biosphere, or direct removal from the air and subsequent storage. Removal of CO_2 from the air is much less efficient than removing it from smokestacks at power plants. For permanent burial the right kind of underground geology is required. Increasing carbon uptake by the land can have additional benefits that increase its economic feasibility. Growing plants for biofuel and then capturing and burying the CO_2 when the fuel is burned produces energy and net reduction of CO_2. Agricultural practices and soil amendments to enhance carbon content of soils also benefit agricultural efficiency. Fertilizing the ocean with trace minerals can increase ocean productivity, but experiments so far indicate that the CO_2 thus taken up is not stored very long in the ocean, and thus is not effective for mitigation of warming. It is unclear whether these approaches can be scaled up enough to be effective in offsetting the increased production of CO_2 by burning of coal, oil, and natural gas. CO_2 removal strategies address the root cause of human-induced warming, and introduce fewer additional risks, but they are expensive, slow and may produce fairly modest results in the near term.

If we continue to alter the atmosphere in the future at an accelerating rate, and the climate is as sensitive as some models suggest, then within a century we could produce a climate on Earth that would be warmer than any in more than a million years. Moreover, the rate of temperature

increase would be very large by natural standards and would make it difficult for plants, animals, and humans to adapt. Because of the long time scale of perturbations in the carbon cycle, once a CO_2-induced warming is initiated, it is essentially permanent from a human perspective. Also, the full warming from a given CO_2 increase does not appear for decades after the CO_2 injection, so that one cannot wait until a "dangerous" 2°C or greater warming has occurred to begin actions to mitigate further warming. Climate science thus has the important challenge of trying to predict the global and regional consequences of human-induced warming as far into the future and with as much detail as possible, both to illustrate the benefits of mitigation and to inform strategies for adaptation to future warming, some of which is already inevitable.

EXERCISES

1. Suppose that a volcanic eruption gives rise to a stratospheric aerosol cloud that changes the instantaneous Earth energy balance by 4 W m^{-2}. The cloud persists unchanged for 2 years. If the heat capacity of the climate system on this time scale is equivalent to a layer of water 50 m deep and the sensitivity of the climate is characterized by a sensitivity parameter $\lambda_R = 1$ K (W $m^{-2})^{-1}$, what is the surface temperature anomaly produced by the aerosol cloud at the end of the 2-year period? What would the temperature response be if the aerosol cloud remained forever? What fraction of this long-term equilibrium response is achieved after 2 years?
2. Consider a situation as in problem 1, except assume that the forcing from the aerosol cloud begins at 4 W m^{-2} but then decreases exponentially with an *e*-folding time of 2 years. Forcing = 4 W m^{-2} exp (–t/2 years). What is the temperature response after 2 years?
3. If the tropical SST is raised by 2°C from 299 to 301 K, and the lapse rate follows the moist adiabatic profile, estimate by how much the temperature at 300 mb will increase?
4. A 1-km-thick layer of the atmosphere at about 55-km altitude is heated by absorption of solar radiation by ozone at a rate that would warm the layer by 10°C day^{-1}. In equilibrium, this solar heating is balanced by longwave cooling. The air density in the layer is about 4×10^{-4} kg m^{-3}. The outgoing longwave radiation is about 240 W m^{-2} on which the stratosphere at this altitude is assumed to have very little effect.
   a. What is the broadband longwave emissivity of this stratospheric layer if it has a radiative equilibrium temperature of 280 K? The emissivity is the ratio of the actual emission from the layer to that of a black body at the same temperature, ε = (emission/σT^4). Assume local thermodynamic equilibrium so that the longwave emissivity of the layer is equal to its absorptivity.

b. The emissivity of the layer depends primarily on the CO_2 concentration, which was initially 300 ppmv. The CO_2 is doubled to 600 ppmv and the climate finds a new equilibrium. The albedo of the planet is assumed to remain constant during this climate change, so that the emission temperature of the planet is unchanged as a result of doubling CO_2. If the emissivity of the air increases approximately as the natural logarithm of the CO_2 concentration so that the new emissivity is 112% of the original one, what will be the new radiative equilibrium temperature of the stratosphere in the doubled CO_2 climate?

5. Suppose we can assume that the climate system has an effective heat capacity equivalent to that of 100 m of ocean, but the climate sensitivity can be either $\lambda_R = 0.5$ or 1.0 K/(W m^{-2}), and we do not know which. A climate forcing is applied that increases linearly with time as $Q = Q_t t$, where $Q_t = 4$ W m^{-2} in 50 years. If the measurement uncertainty for global mean temperature is 0.5°C, how many years will it be before we could distinguish whether the climate sensitivity is characterized by $\lambda_R = 0.5$ or 1.0 K/(W m^{-2})? That is, when would the temperature for the more sensitive climate exceed that of the less sensitive climate by 0.5°C? What are the temperature perturbations of the global climate for the two sensitivities when they differ by 0.5°C? If the climate forcing is held constant at its value when the two responses become distinguishable, what will be the equilibrium response for each sensitivity? *Hint*: Start by assuming that the time in question is significantly longer than the response time τ_R, so that the exponential transient in the solution (13.9) can be ignored. Determine a posteriori whether this assumption is justified.